Developing deep LSTMs with later temporal attention for predicting COVID-19 severity, clinical outcome, and antibody level by screening serological indicators over time

Jiaxin Cai, Yang Li, Baichen Liu, Zhixi Wu, Shengjun Zhu, Qiliang Chen, Qing Lei, Hongyan Hou, Zhibin Guo, Hewei Jiang, Shujuan Guo, Feng Wang, Shengjing Huang, Shunzhi Zhu, Xionglin Fan, and Shengce Tao.

***Abstract*— Objective: The clinical course of COVID-19, as well as the immunological reaction, is notable for its extreme variability. Identifying the main associated factors might help understand the disease progression and physiological status of COVID-19 patients. The dynamic changes of the antibody against Spike protein are crucial for understanding the immune response. This work explores a temporal attention (TA) mechanism of deep learning to predict COVID-19 disease severity, clinical outcomes, and Spike antibody levels by screening serological indicators over time.**

Methods: We use feature selection techniques to filter feature subsets that are highly correlated with the target. The specific deep Long Short Term Memory (LSTM) models are employed to capture the dynamic changes of disease severity, clinical outcome, and Spike antibody level. We also propose deep LSTMs with a TA mechanism to emphasize the later blood test records because later records often attract more attention from doctors.

Results: Risk factors highly correlated with COVID-19 are revealed. LSTM achieves the highest classification accuracy for disease severity prediction. Temporal Attention Long Short Term Memory (TA-LSTM) achieves the best performance for clinical outcome prediction. For Spike antibody level prediction, LSTM achieves the best permanence.

Conclusion: The experimental results demonstrate the effectiveness of the proposed models. The proposed models can provide a computer-aided medical diagnostics system by simply using time series of serological indicators.

***Index Terms*— COVID-19, clinical decision making, deep learning, ensemble learning, attention mechanism, Long Short Term Memory.**

This work is supported by the Natural Science Foundation of Fujian Province (2023J05083,2022J011396,2023J011434). Jiaxin Cai, Yang Li, Baichen Liu, and Zhixi Wu are co-first authors. Corresponding authors: Jiaxin Cai and Shengce Tao.

Jiaxin Cai and Shengjun Zhu are with the School of Mathematics and Statistics, Xiamen University of Technology, Xiamen, China (e-mail: caijiaxin@xmut.edu.cn; 19359446568@163.com;).

Yang Li, Hewei Jiang, Shujuan Guo, and Shengce Tao are with Shanghai Center for Systems Biomedicine, Key Laboratory of Systems Biomedicine (Ministry of Education), Shanghai Jiao Tong University, Shanghai, China (e-mail: liyang202202@163.com; jhw622@sjtu.edu.cn; shjguo@sjtu.edu.cn; taosc@sjtu.edu.cn).

Baichen Liu, Zhixi Wu, Qiliang Chen, Zhibin Guo, and Shunzhi Zhu are with the School of Computer and Information Engineering, Xiamen University of Technology, Xiamen, China (e-mail: 715603015@qq.com; yanmu203@qq.com; 643362009@qq.com; zhibinguo1@163.com; szzhu@xmut.edu.cn).

Qing Lei, Hongyan Hou, and Feng Wang are with the Tongji Hospital, Tongji Medical College, Huazhong University of Science and Technology, Wuhan, China (e-mail: leiqinghust@163.com; houhongyan89@163.com; fengwang@tjh.tjmu.edu.cn).

Shengjing Huang is with the School of Electrical Engineering and Automation, Xiamen University of Technology, Xiamen, China (e-mail: 1803547326@qq.com.

Xionglin Fan is with the School of Basic Medicine, Tongji Medical College, Huazhong University of Science and Technology, Wuhan, China (e-mail: xlfan@hust.edu.cn).

I. Introduction

Coronavirus Disease 2019 (COVID-19) is caused by Severe Acute Respiratory Syndrome Coronavirus 2 (SARS-CoV-2), a beta coronavirus [1]. By July 2022, over 569,068,506 cases of COVID-19 had been reported, with almost 6,382,625 deaths, which brought unbearable pressure on global healthcare systems (https://coronavirus.jhu.edu/map.html). Under the pressure of the pandemic, developing reliable and effective diagnostic techniques is going to be crucial. To mitigate the burden on the healthcare system, machine learning (ML) and deep learning (DL) have been widely applied for early detection, diagnosis, disease progression monitoring, and other issues of COVID-19. Chest Computed Tomography (CT) is a high-sensitivity analysis tool for the early diagnosis of COVID-19, and DL has a high capability of feature extraction in CT image detection. Saood et al. [2] proposed SegNet and U-NET models to detect and label infected tissues on lung CT images of COVID-19 patients. Li et al. [3] developed a COVNet model to detect COVID-19 patients, which can effectively extract and select the hidden pathological features in the CT images. However, CT is expensive and delivers high radiation doses (approximately 2-20 mSv) [4]. Therefore, other auxiliary diagnostic techniques are imperative.

The serological indicators are highly correlated with the disease progression and physiological status of patients. Some crucial serological indicators that help diagnose COVID-19 cases have been confirmed, and the diagnostic performance is comparable to RT-PCR and chest CT. The Diagnosis and

Treatment Protocol for COVID-19 [1], which is issued by the National Health Commission of China, points out that the routine diagnosis of COVID-19 should include the examination of total peripheral blood leukocytes, lymphocyte count, liver enzyme, lactic dehydrogenase (LDH), muscle enzyme, Myoglobin, Troponin, Ferritin, C-reactive protein (CRP), Procalcitonin (PCT), D-dimer, and peripheral blood lymphocyte count. It also points out that the general treatment of COVID-19 should include the examination of CRP, liver enzyme, and myocardial enzyme. So blood tests are part of the routine diagnosis and standard of treatment for the COVID-19 patient. Kukar et al. [5] provided an XGBoost model to make a diagnosis based on blood routine data. Soltan et al. [6] developed two early-detection models trained using health care data (laboratory tests, blood gas measurements, and vital signs), to screen COVID-19 patients in the emergency department . However, current works ignore the importance of considering time-varying information on serological indicators that change as the disease progresses. The experience of developing a diagnostic model for COVID-19 using the temporal information of routine blood test data is still not readily available. Additionally, several studies [7]–[9] suggested that immune responses are related to disease severity. Yan et al. [10] found high IgG antibody concentration in severe COVID-19 patients. Guo et al. [11] observed that the IgG antibody concentration of severe COVID-19 patients was higher than that of moderate COVID-19 patients. However, serological indicators associated with Spike antibody levels are still not clear. For COVID-19, the clinical course, as well as the immunological reaction, is notable for its extreme variability. Identifying the main associated serological indicators might help assess the status of the disease.

Against this background, our work reveals several risk predictors associated with disease severity and clinical outcome in COVID-19 patients from serum indices. We design specific temporal deep learning models for predicting disease severity and clinical outcome by time series of serological markers. Later records of disease observations usually attract more attention from doctors. Specifically, we focus on modeling the time characteristics in clinical outcome prediction and propose a novel neural network architectural unit, which we term the "Temporal Attention" (TA) block, to emphasize the later blood test records which are more valuable and suppress the earlier records which are less valuable. Moreover, we utilize the ensemble learning models to screen critical predictors associated with the Spike antibody level from serum indices, and the Spike antibody level prediction model is constructed using time-series and non-time-series data, respectively.

- We introduce temporal information into the serological indicators based COVID-19 prediction problem. This study not only screens key serological indicators that affect the progression of COVID-19 but also helps the clinician identify COVID-19 patients with the potential risk of developing into severe/critical illness and death at an early stage.
- We propose a later temporal attention mechanism for deep COVID-19 networks. We integrate the proposed TA block into the COVID-19 network architecture. The proposed TA block significantly improves the performance of COVID-19 network with a minimal increase in computational cost. The proposed TA block is effective in enhancing global temporal dependencies.
- We reveal the clear correlation between COVID-19 severity and Spike antibody level and find the key serological indicators associated with Spike antibody level. We utilize ensemble learning models to screen Top-30 key serological indicators and construct regression models to predict the concentration of Spike antibody, which can help doctors assess the patient's condition.

The rest of this paper is structured as follows. Section 2 describes the sources of the materials, and Section 3 outlines the method's details. The experimental results and the discussion are presented in Sections 4 and 5, respectively. Finally, the conclusions and future works are given in Section 6.

II. Participants and Data Recording

The study is conducted in accordance with the Declaration of Helsinki, and the protocol is approved by the Ethics Committee of Tongji Hospital, Huazhong University of Science and Technology, China. We collect retrospective data on COVID-19 patients admitted to Tongji Hospital, Wuhan, China, from January/2020 to May/2020. Each patient has one admission record and one discharge record. All patients are hospitalized. There are no outpatients among patients. For each patient, we test the serum indices at admission time and get the admission serological test record (sample). During hospitalization (except for admission time and discharge time), patients undergo several serological tests at various time points and frequencies, and several serological test records are collected. For each patient, we test the serum indices at the time of discharge and get the discharge serological test record. There are no patients who are re-hospitalized or re-visiting patients. And there are no missing admission records or missing discharge records. Therefore, each patient has only one admission blood test record, only one discharge blood test record, and several during-hospitalization blood test records. The total number of patients is 1054. Since the number of the serological assessment records of each patient varies, the total number of blood test samples (records) from all patients is 12,621. The serological indicators for the blood test are listed in APPENDIX A. The S1_IgG levels are also tested at the blood test time for patients. The clinical characteristics of patients are also collected. Table I lists the descriptive statistics for the clinical characteristics of patients. However, some blood test samples contain missing data. There are no blood test data outside of routine care.

For the variable "disease severity," asymptomatic infection or mild are replaced with 0, and severe or critical are replaced with 1. We provide the reasons behind this choice. The Diagnosis and Treatment Protocol for COVID-19 in China [1] individually suggests the IL-6, CRP, ferritin, and D-Dimer indicators for indicating COVID-19 patients with severe or critical disease. These indicators are used as warning indicators for the transition from asymptomatic infection or mild disease

to severe or critical disease. In the Protocol [1], patients with severe and critical disease share the same supporting treatment plan; asymptomatic infected patients and mild patients share the same general treatment guidelines. So we separate the disease severity into asymptomatic/mild and severe/critical to meet practical clinical needs. The tested patients are assessed as asymptomatic/mild or severe/critical based on comprehensive symptoms according to the Protocol [1]. For the variable "clinical outcome," survivor is replaced with 0, and non-survivor is replaced with 1. The data is made suitable for analysis by preprocessing. Fig. 1 illustrates the procedure of the data preprocessing. Finally, we obtain dataset A, dataset B, and dataset C.

TABLE I: The descriptive statistics for clinical characteristics of the diagnosed COVID-19 patients. The continuity variables are expressed by the mean (s.d.), and the categorical variables are expressed as numbers (percentages).

Variable	COVID-19 Case (n)
Sex:	
female	528 (50.2%)
male	523 (49.8%)
Age (year)	60.1 (15.3)
Outcome:	
non-survivor	79 (7.5%)
survivor	972 (92.5%)
Severity:	
asymptomatic infection	4 (0.4%)
critical	513 (48.9%)
mild	398 (37.9%)
severe	135 (12.9%)
High blood pressure (HBP) :	
no	660 (62.8%)
yes	391 (37.2%)
Diabetes mellitus (DM) :	
no	859 (81.7%)
yes	192 (18.3%)

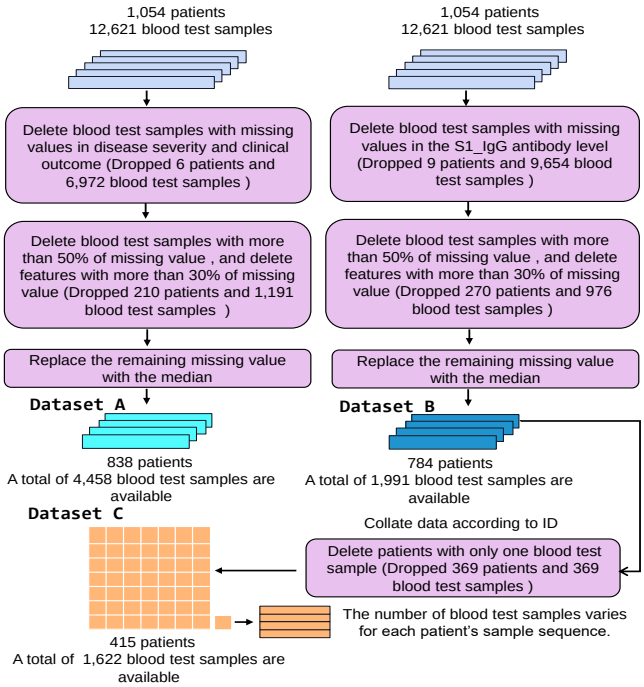

Fig. 1. The procedure of data preprocessing.

III. METHODS

A. Temporal Attention Block

The advantage of LSTM is that it can handle long-term dependencies, but the disadvantage is that it is ineffective in capturing potential time dependencies between different observations. In the medical field, doctors tend to focus on later records of disease observations, which can provide a quick snapshot of the patient's recent health status. Combining information from different periods to build a holistic representation of disease progression is crucial for guiding decisions regarding patient care and treatment. We anticipate explicitly enhancing the temporal dependencies of temporal neural networks to enhance the networks' sensitivity to different time. To this end, we present the Temporal Attention (TA) block into the temporal deep learning architecture by adding different weights on the neurons so that the later blood test records have more attentions.

Fig. 2 illustrates the proposed TA block. Given a time series feature map X, we induce an attention map over the input feature map to focus on the important position. The initial attention map $U \in \mathbb{C}^{H\times W}$ is expressed as Equation 1.

$$U = \begin{bmatrix} u_{11} & u_{12} & \cdots & u_{1W} \\ u_{21} & u_{22} & \cdots & u_{2W} \\ \cdots & \cdots & \cdots & \cdots \\ u_{H1} & u_{H2} & \cdots & u_{HW} \end{bmatrix} \tag{1}$$

Here, H denotes the time length of X; W denotes the feature number of X. The TA block implicitly assumes that the time gaps between adjacent time points are equal. Initially, each feature of X has the same attention weight; and for each time point of X, the attention weight equal the time, that is to say $U_{h,w} = h$ for all w. As expressed in Equation 2, we apply the softmax function on the initial attention map U to generate $\widetilde{U}$, exponentially enhancing the attention weights of the latter records that are more correlated with clinical outcome. Finally, the attention map $\widetilde{U}$ is applied on the input feature map X to generate the output $\widetilde{X}$, which can be fed into the next layer of the network. The proposed TA block provides an interpretable manner to enhance the global time dependence. It imposes a very slight increase in computational burden.

$$softmax(U_{h,.}) = \frac{exp(U_{h,.})}{\sum_{h=1}^{H} exp(U_{h,.})} \tag{2}$$

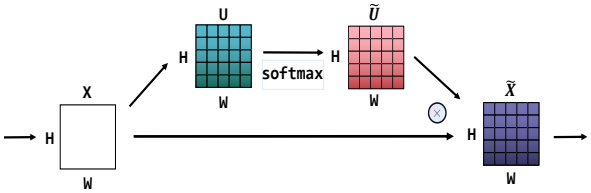

Fig. 2. The proposed temporal attention block.

B. Predictor Architecture

We treat both disease severity prediction and clinical outcome prediction as classification problems. Furthermore, we

treat the Spike antibody level prediction as a regression problem.

1) Task 1: Disease severity prediction: The proposed model consists of eight layers: an LSTM layer, a batch normalization layer, a flattened layer, a fully-connected network layer, a dropout layer, and a sigmoid layer. The first layer is an LSTM layer with 160 hidden units; the nonlinear activation function of the LSTM layer is rectified linear element (ReLU). The second layer is a batch normalization layer, which can adjust the activation mean and scale to speed up the network's training. The third layer is a flattened layer, which flattens the input. Then, we add a dropout layer behind the flattened layer. The response of the dropout layer is fed to a fully-connected layer with one unit, connected by a sigmoid layer for predicting the output. The binary cross-entropy is employed as the loss function. The Adam optimizer is employed, the epoch is 20, and the batch size is 128.

2) Task 2: Clinical outcome prediction: The proposed model consists of ten layers: a TA block layer, an LSTM layer, a batch normalization layer, a flattened layer, two fully-connected network layers, a dropout layer, and a sigmoid layer. The first layer is a TA block layer where the attention map $\widetilde{U}$ is applied on the feature map X to generate a new feature map $\widetilde{X}$ with global temporal information. The second layer is an LSTM layer with 160 hidden units and utilizes $ReLU$ as the non-linear activation function. The third layer is a batch normalization layer. The fourth layer is the first full-connected layer with 80 units. The fifth layer is a flattened layer, which flattens the input. Then, we add a dropout layer behind the flattened layer. The response of the dropout layer is fed to the second full-connected layer with one unit, which is connected by a sigmoid layer for predicting the output. To tackle the class imbalance problem, the weighted binary cross-entropy is employed as the loss function. The Adam optimizer is employed; the epoch is 75, and the batch size is 128.

Here is the explanation of why the TA block is not used in Task 1. By adding different weights to different time, TA gives more attention to later records. In our data, the variable "disease severity" denotes the most serious disease condition during the whole period from admission to discharge. Such most serious disease condition often occurs in the middle time of hospitalization. There is no significant relation between the variable "disease severity" and the latest records. However, the later records have greater significance for clinical outcome prediction, providing a quick overview of the patient's recent overall health status. Therefore, we only use the TA block in Task 2.

3) Task 3: Spike antibody level prediction: We build Spike antibody level prediction models using time-series and non-time-series data, respectively. While using non-time-series data, we propose a Spike antibody level prediction model based on CatBoost. For CatBoost, the maximum depth is 6, the learning rate is 0.01, the subsample ratio of the training instances is 0.71, the minimum sum of instance weight (hessian) needed in a child is 1, and the tree estimator number is 10000. While using time-series data, we propose a temporal deep learning model based on LSTM. The model consists of six layers: a Masking layer, an LSTM layer, two dropout layers, and two fully-connected network layers. The first layer is a Masking layer, which can skip and ignore certain timesteps in sequence inputs. The second layer is an LSTM layer with 100 hidden units. Then, the first dropout layer is introduced to take the response of the LSTM layer as input. It prevents overfitting by nullifying the contribution of some neurons toward the next layer; the dropout ratio is 0.5. The fourth layer is a fully-connected layer with three units. Then, the second dropout layer is added behind the fully-connected network layer, and the dropout ratio is 0.2. The last layer is a fully-connected network layer with one unit. The mean absolute error (MAE) is employed as the loss function. The Adam optimizer is used, the epoch is 25, and the batch size is 16.

The architectures of the severity prediction model, clinical outcome prediction model, and time-series based Spike antibody level prediction model are illustrated in Fig. 3.

C. The whole framework

Dataset A, Dataset B, and Dataset C are used for Task 1, Task 2, and Task 3 respectively. For Dataset A, Dataset B, and Dataset C, each dataset is randomly separated into a training set and a test set. The dataset is split by patient ID. The Train-Test split ratio is 80/20. A training/test sample corresponds to a specific patient. A training/test sample is a sequence or a time series that contains the corresponding patient's all blood test samples (records) collected at different time. The blood test samples contained in training set and that in the test set belong to different patients. Therefore, multiple records of one patient only appear in the training set or the test set. So there is no train-test contamination. All sequences are normalized to that of a length of 14 by temporally sampling. We compute the mean and standard deviation of the training set and then perform the Z-score standardization on the training set. Then we utilize a 5-fold cross-validation (CV) to perform feature selection on the training set. The original features include the tested serological indicators, sex, age, HBP and DM. Based on the selected features, we then perform hyperparameter tuning by a 5-fold CV on the training set and get the best trained model with the maximal CV accuracy. We perform the same Z-score standardization on the test set by the same mean and standard deviation which are computed from the previous training set. Based on the selected features obtained from the training set, we adopt the best trained model on the test set to get the evaluation results.

We utilize least absolute shrinkage and selection operator with CV (LassoCV), elastic net with CV (ElasticNetCV), and random forest (RandomForest) to find the Top-10 features associated with disease severity and clinical outcome respectively. Further, we iteratively remove one least significant feature from the Top-10 features by retraining the feature selection and classification models to explore the best feature number. For the Spike antibody level prediction, we utilize CatBoost, XGBoost, and LightGBM to find the Top-30 features. For the disease severity and clinical outcome prediction, the performance of each classification model is evaluated by classification accuracy, F1-score, Area Under Curve (AUC), and BEP (Break-Even Point, precision = recall), respectively. We consider classification accuracy as the

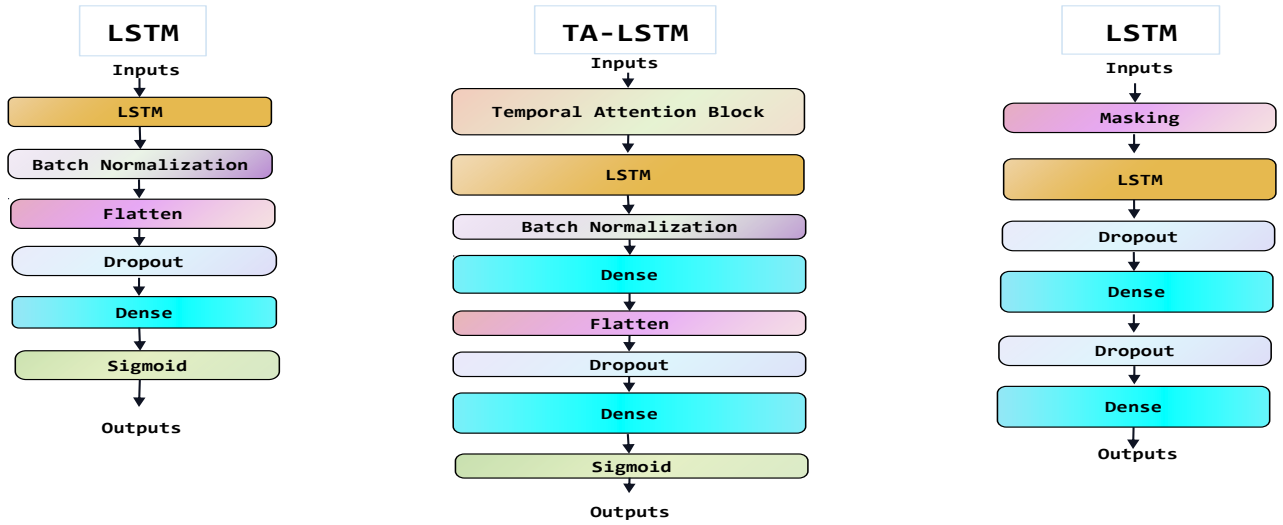

Fig. 3. The architectures of the proposed models. Left: COVID-19 disease severity prediction model. Middle: COVID-19 clinical outcome prediction model. Right: Time-series based Spike antibody level prediction model.

primary quality metric. For the Spike antibody level prediction, the performance of each regression model is evaluated by average squared error (MSE), root mean squared error (RMSE), MAE, and coefficient of determination (R^2), respectively. We consider R^2 as the primary quality metric. All experiments are implemented in Python 3.6 with TensorFlow 1.14.0 on a computer with CPU Intel Xeon Gold 6138 @ 2.00GHz (40 cores) and GPU NVIDIA RTX2080Ti. All descriptive statistics are performed using RStudio, and $p<0.05$ is considered as statistically significant.

IV. Experimental Result

A. Task 1: Disease severity prediction

Fig. 4 shows the Top-10 features associated with disease severity. As shown in Fig. 5, the LassoCV-ElasticNetCV LSTM algorithm achieves the optimal classification accuracy of 0.79048 when the number of features is 6. LassoCV-ElasticNetCV denotes that LassoCV and ElasticNetCV give the same feature subset. The best feature subset includes LDH, Absolute value of monocyte (Mono%), Albumin (ALB), Percentage of lymphocytes (LYMPH%), DM and Sex. Table II shows the descriptive statistics of the optimal feature subset; p of all features are less than 0.001. Fig. 6 shows the confusion matrices of the classification algorithms, and Table III shows the results of performance evaluation. The F1-score is the harmonic mean of precision and recall; a high F1-score indicates a relatively high value for both recall and precision. For LassoCV-ElasticNetCV LSTM, the Class 0 prediction F1-score is 0.78641, the Class 1 prediction F1-score is 0.79439, and the weighted average F1-score is consistently larger than that of other algorithms. In Fig. 7, the LassoCV-ElasticNetCV LSTM algorithm achieves the highest AUC (0.84302). The results demonstrate the effectiveness of the proposed specific LSTM model for predicting COVID-19 severity.

TABLE II: Descriptive statistics of the optimal feature subset for severity prediction.

COVID-19 Sample (n)	asymptomatic infection and mild 1391	severe and critical 3067	p
LYMPH%	25.3 (10.5)	15.5 (11.4)	<0.001
LDH	227 (78.5)	334 (202)	<0.001
ALB	36.8 (4.57)	33.1 (5.06)	<0.001
Mono%	8.96 (3.02)	7.11 (3.44)	<0.001
COVID-19 Patient (n)	417	421	
DM			<0.001
no	357 (86.0%)	320 (76.0%)	
yes	60 (14.0%)	101 (24.0%)	
Sex			<0.001
female	241 (57.8%)	185 (43.9%)	
male	176 (42.2%)	236 (56.1%)	

TABLE III: Performance evaluation results of the algorithms with the highest severity prediction accuracy. **Weighted avg**: averaging the support-weighted mean per label.

	Precision	**Recall**	**F1-score**
LassoCV-ElasticNetCV LSTM			
0	0.75701	0.81818	**0.78641**
1	0.82524	0.76577	0.79439
Weighted avg	0.79308	0.79048	**0.79063**
LassoCV-ElasticNetCV 1D-CNN			
0	0.77551	0.76768	0.77157
1	0.79464	0.80180	0.79821
Weighted avg	0.78562	0.78571	0.78565
LassoCV-ElasticNetCV 2D-CNN			
0	0.82716	0.67677	0.74444
1	0.75194	0.87387	**0.80833**
Weighted avg	0.78740	0.78095	0.77821
LassoCV-ElasticNetCV KNN			
0	0.68376	0.80808	0.74074
1	0.79570	0.66667	0.72549
Weighted avg	0.74293	0.73333	0.73268

B. Task 2: Clinical outcome prediction

Fig. 8 shows the Top-10 features associated with clinical outcome. Fig. 9 shows that the LassoCV-ElasticNetCV TA-LSTM algorithm achieves an optimal classification accuracy of 0.99048 when the feature number is 5. The best feature subset

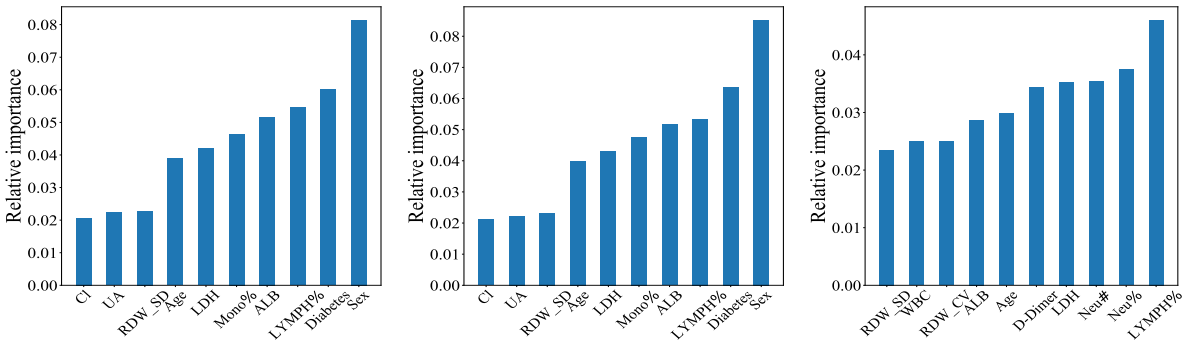

Fig. 4. Top-10 features for disease severity prediction.
a: features selected by LassoCV. b: features selected by ElasticNetCV. c: features selected by RandomForest.

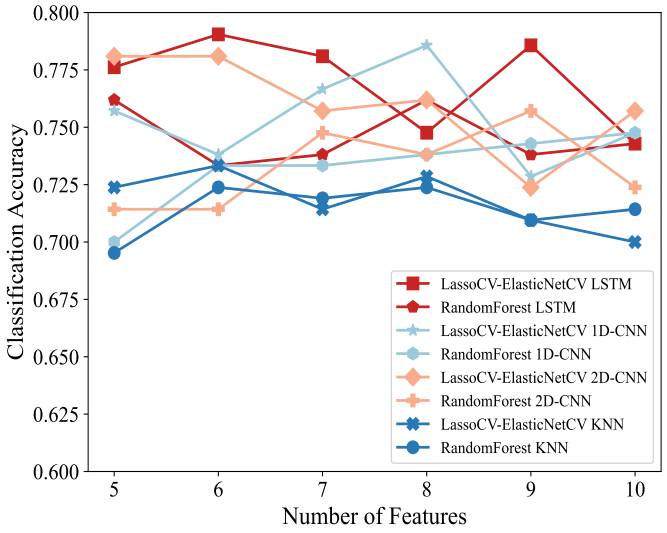

Fig. 5. Severity prediction accuracies corresponding to different numbers of selected features. The highest accuracy for LSTM is 0.79048, for 1D-CNN is 0.78571, for 2D-CNN is 0.78095, and for KNN is 0.73333.

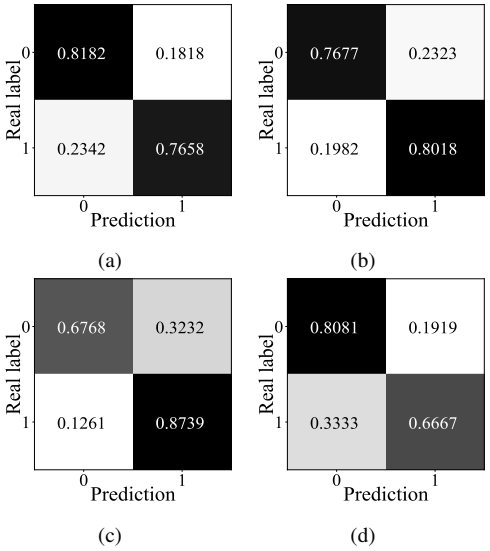

Fig. 6. Confusion matrices of the algorithms with the highest severity prediction accuracy. a: LassoCV-ElasticNetCV LSTM. b: LassoCV-ElasticNetCV 1D-CNN. c: LassoCV-ElasticNetCV 2D-CNN. d: LassoCV-ElasticNetCV KNN.

includes LDH, Mono%, ALB, LYMPH%, DM, and Sex. As can be seen from Fig. 10 and Table IV, introducing the TA block into time series models leads to significant performance improvement with a small increase in computational cost. The results demonstrate the effectiveness of the TA block in enhancing global temporal dependencies. Fig. 11 shows the confusion matrices of the classification algorithms; Table V shows the performance evaluation results. For the LassoCV-ElasticNetCV TA-LSTM algorithm, the Class-0 prediction F1-score is 1.00000 , the Class-1 prediction F1-score is 0.88235 , and the weighted average F1-Score is larger than that of other algorithms. As shown in Fig. 7, LassoCV-ElasticNetCV TA-LSTM achieves the largest AUC. Table VI shows the descriptive statistics of the optimal feature subset; for all features, p is less than 0.001. As shown in Fig. 12, TA-LSTM can predict 10 days in advance with an average classification accuracy of 90%. The results demonstrate the effectiveness of TA block in enhancing global temporal dependencies with a minimal increase in computational cost. The temporal attention based deep learning models outperform KNN using non-time-series data and the traditional temporal deep learning models.

TABLE IV: Performance comparison of outcome prediction models under different random seeds. (Feature subset: Mono%, INR, Neu#, ALB, hs-CRP, PLT, Urea, and LDH)

Seed	Method	Classification accuracy	Training time
5	LSTM	0.98095	45.36478 s
	TA-LSTM	0.99047	50.91895 s
	1D-CNN	0.96190	17.53014 s
	TA-1D-CNN	0.97140	16.08220 s
10	LSTM	0.97143	39.28945 s
	TA-LSTM	0.99047	42.23910 s
	1D-CNN	0.95710	6.33886 s
	TA-1D-CNN	0.97140	14.66752 s
15	LSTM	0.96667	50.27024 s
	TA-LSTM	0.98571	44.94084 s
	1D-CNN	0.97620	9.81103 s
	TA-1D-CNN	0.95240	5.99308 s

C. Task 3 (Antibody level prediction)

Table IX shows the Top-30 features associated with the Spike antibody level. The three feature selection methods share the same Top-3 features: age, RDW_CV,and PLT. Table VII and Table VIII show the performance evaluation results of

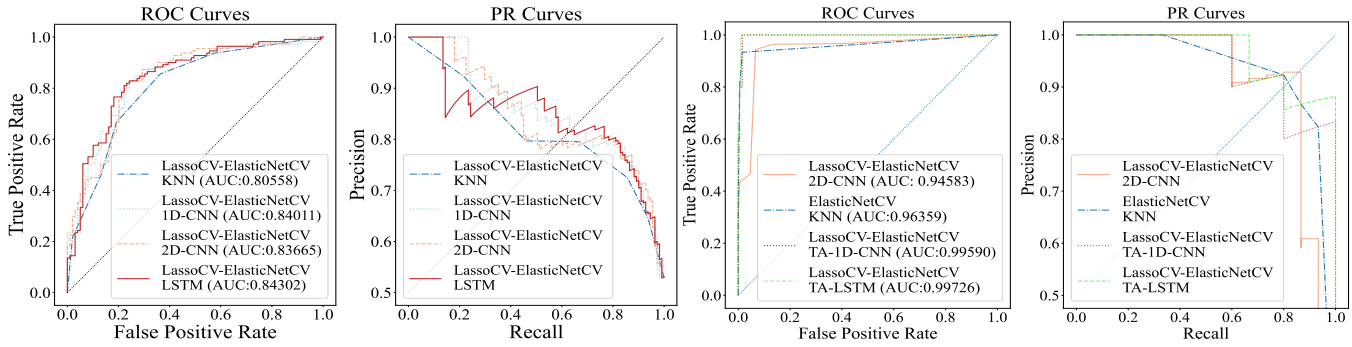

Fig. 7. ROC and PR curves of the classification models with the highest classification accuracy. a: Comparison of ROC curves regarding disease severity prediction. b: Comparison of PR curves regarding disease severity prediction. c: Comparison of ROC curves regarding clinical outcome prediction. d: Comparison of PR curves regarding clinical outcome prediction.

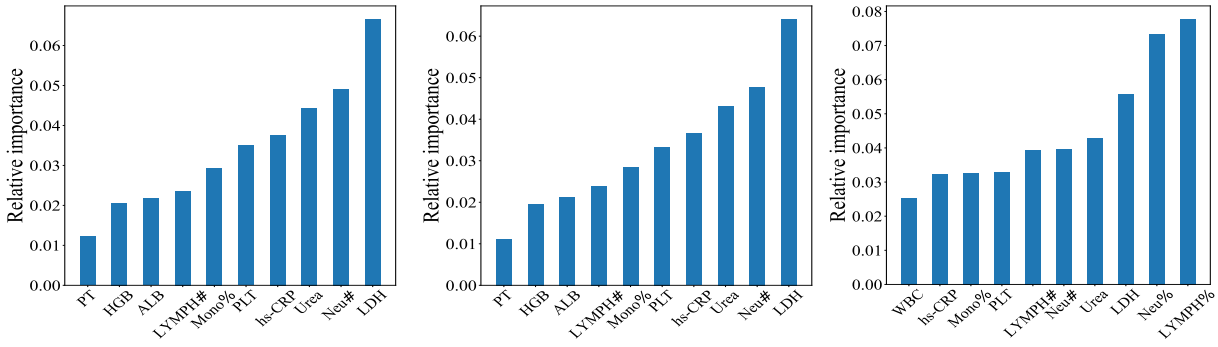

Fig. 8. Top-10 features for clinical outcome prediction. a: feature subset screened by LassoCV. b: feature subset screened by ElasticNetCV. c: feature subset screened by RandomForest.

TABLE V: Regarding clinical outcome prediction, performance evaluation results of the algorithms with the highest classification accuracy. **Weighted avg**: averaging the support-weighted mean per label.

	Precision	Recall	F1-score
LassoCV-ElasticNetCV LSTM			
0	0.98974	0.98974	0.98974
1	0.86667	0.86667	0.86667
Weighted avg	0.98095	0.98095	0.98095
LassoCV-ElasticNetCV TA-LSTM			
0	1.00000	0.98974	**0.99485**
1	0.88235	1.00000	**0.93750**
Weighted avg	0.99160	0.99048	**0.99075**
LassoCV-ElasticNetCV 1D-CNN			
0	0.98953	0.96923	0.97927
1	0.68421	0.86667	0.76471
Weighted avg	0.96772	0.96190	0.96395
LassoCV-ElasticNetCV TA-1D-CNN			
0	1.00000	0.97436	0.98701
1	0.75000	1.00000	0.85714
Weighted avg	0.98214	0.97619	0.97774
LassoCV-ElasticNetCV 2D-CNN			
0	0.98477	0.99487	0.98980
1	0.92308	0.80000	0.85714
Weighted avg	0.98036	0.98095	0.98032
LassoCV-ElasticNetCV KNN			
0	0.98477	0.99487	0.98980
1	0.92308	0.80000	0.85714
Weighted avg	0.98036	0.98095	0.98032

TABLE VI: Descriptive statistics of the optimal feature subset in the clinical outcome prediction task.

COVID-19 Sample (n)	non-survivor 726	survivor 3732	p
Neu#	11.0 (6.19)	5.29 (3.60)	<0.001
hs-CRP	90.2 (84.0)	25.4 (42.1)	<0.001
PLT	140 (102)	231 (96.1)	<0.001
Urea	12.2 (8.47)	5.77 (3.93)	<0.001
LDH	497 (295)	263 (114)	<0.001

each algorithm. Among models using non-time-series data, the combination of CatBoost feature selection and CatBoost prediction achieves the largest R^2 of 0.071 . Among models using time-series data, the combination of CatBoost feature selection and LSTM prediction achieves the highest R^2 of 0.519, and the lowest MSE, RMSE, and MAE. The R^2 of models using time-series data are higher than that of models using non-time–series data. LSTM achieves the best performance. The time-series model is more suitable than non-time-series model for antibody level prediction task.

Age, RDW_CV, Platelet count (PLT), LDH, eGFR(CKD-EPI), LYMPH#, RDW_SD, PCT, and TCHO are the Top-9 significant features obtained by CatBoost. We train the LSTM model using these 9 features and obtain a fitting curve.The fitting curve is shown in Fig. 13. The fitting curve shows a close alignment between the prediction and the true. The LSTM model using features selected by CatBoost show a

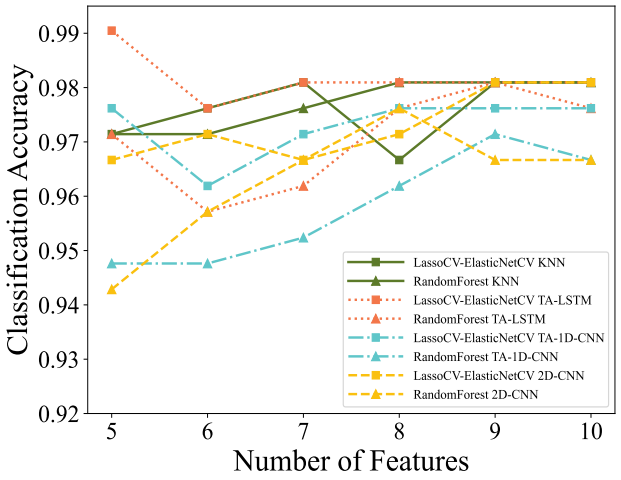

Fig. 9. Clinical outcome classification accuracies corresponding to different numbers of features. The highest classification accuracy for LSTM is 0.98095, for TA-LSTM is 0.99048, for 1D-CNN is 0.96190, for TA-1D-CNN is 0.97619, for 2D-CNN is 0.98095, and for KNN is 0.98095.

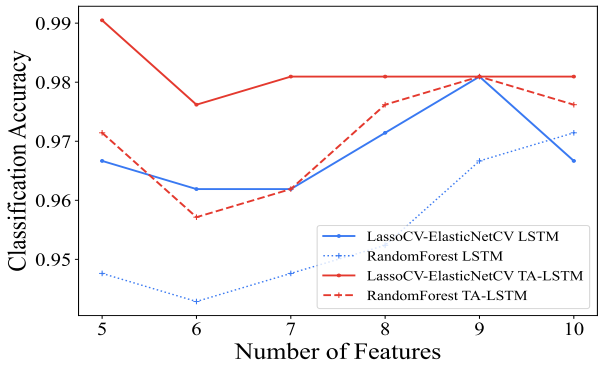

(a)

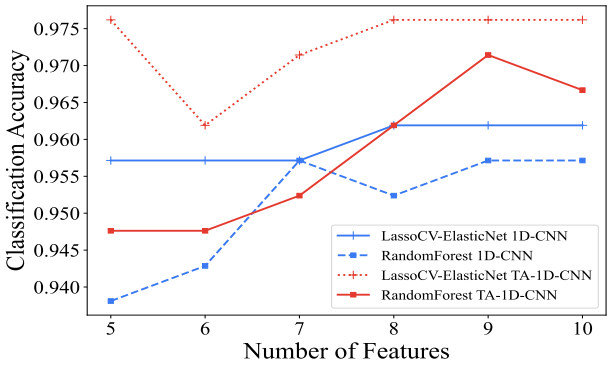

(b)

Fig. 10. Comparison of the time series models and the models with TA in clinical outcome classification accuracy. a: Comparison of LSTM and TA-LSTM. b: Comparison of 1D-CNN and TA-1D-CNN.

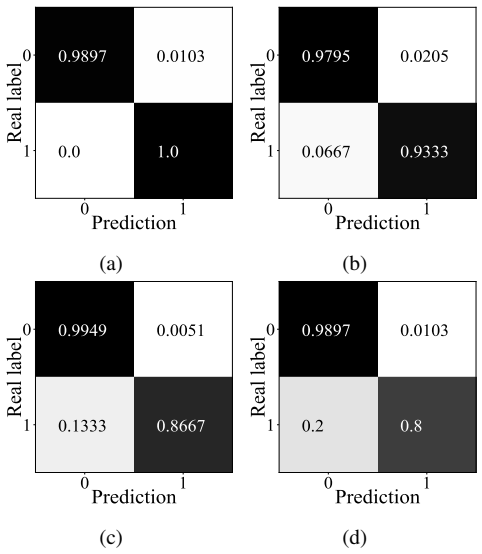

Fig. 11. Regarding clinical outcome prediction, confusion matrices of the classification algorithms with the highest classification accuracy. a: LassoCV-ElasticNetCV TA-LSTM. b: LassoCV-ElasticNetCV TA-1D-CNN. c: LassoCV-ElasticNetCV 2D-CNN. d: LassoCV-ElasticNetCV KNN.

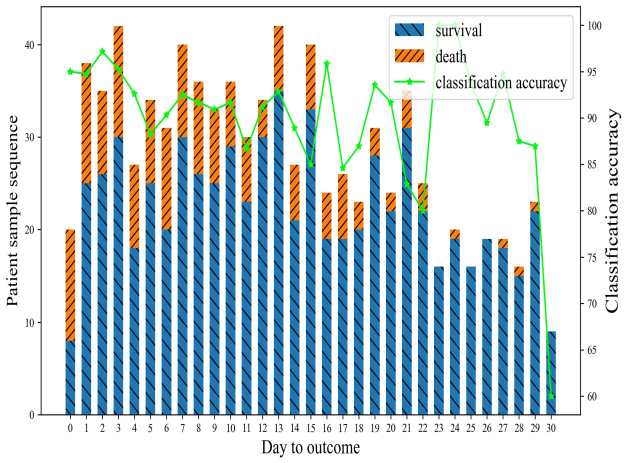

Fig. 12. The clinical outcome prediction performance with respect to the days of advance prediction using the feature subset of Neu#, hs-CRP, PLT, Urea, and LDH.

good fitting performance. Furthermore, as time progresses, the fitting performance of the LSTM model improves gradually. Fig. 13 shows that LSTM has a good effect in predicting Spike antibody level. Fig. 14 shows the scatter distributions between the Spike antibody level and these 9 features. We can observe that there is a linear correlation between Spike antibody level and Age/PCT/eGFR(CKD-EPI)/LYMPH#. We find that Spike antibody level is positively correlated with Age and PCT, and negatively correlated with eGFR(CKD-EPI) and LYMPH#. The scatter distributions of RDW_CV, LDH, and RDW_SD are very similar. This characteristic indicates that RDW_CV, LDH, and RDW_SD may have a mutual effect or a coupled effect on Spike antibody level. These three features may need to be treated as a group factor. Besides, IgG value will fluctuate greatly when these three

features fluctuate slightly. Similarly, Spike antibody level is also sensitivity to the fluctuations of LYMPH#. Moreover, the scatter distributions of PLT and TCHO are also very similar. These two features may synchronously affect Spike antibody level. They may also belong to a group factor.

Our results show a clear correlation between COVID-19 severity and Spike antibody. Zhang et al. [12] shows that the strong immune response to SARS-COV-2 is associated with COVID-19 severity; this robust anti-IgG response contributes to viral clearance and immune-mediated tissue damage. Accordingly, immune-mediated tissue damage directly contributes to the deterioration of the patient's disease; simultaneously, more LDH is released into the blood. Embaby et al. [13] utilized the multivariable analysis of the PLT count as an independent prognostic predictor for mortality. However, previous studies have not well-established the association between PLT and the Spike antibody level. More explorations are required to understand and explain PLT's role in the Spike response. Our results also reveal the relations between Spike antibody level and LDH/PLT. Shankaralingappa et al. [14] found PCT is significantly decreased in COVID-19 patients compared to non-COVID individuals. Our results also indicate that the Spike antibody level positively correlates with PCT. Moreover, Mirijello et al. [15] suggested that low eGFR is a highly relevant prognostic marker for poor prognosis in COVID-19 patients, usually associated with high Spike levels. Our results also indicate that Spike antibody level negatively correlates with eGFR(CKD-EPI). Nader et al. [16] found that LYMPH# is a diagnostic predictor of asymptomatic COVID-19. Our results also indicate a linear relationship between IgG and LYMPH#. Wang et al. [17] found that the severe group's RDW_CV and RDW_SD are significantly higher than those in the moderate group. Our results also reveal the relationships between IgG and RDW_CV/RDW_SD.

TABLE VII: Comparison of different combinations of feature selection methods and regression methods for non-time-series data based Spike antibody levels prediction.

Regression Method	FS Method	MSE	RMSE	MAE	R^2
CatBoost	**CatBoost**	**1.149**	**1.072**	**0.833**	**0.071**
	XGBoost	1.162	1.078	0.840	0.061
	LightGBM	1.150	1.073	0.837	0.070
XGBoost	**CatBoost**	1.188	1.090	0.862	0.040
	XGBoost	1.204	1.097	0.865	0.026
	LightGBM	1.181	1.087	0.863	0.046
LightGBM	**CatBoost**	1.169	1.081	0.860	0.056
	XGBoost	1.180	1.086	0.859	0.047
	LightGBM	1.170	1.081	0.860	0.055

TABLE VIII: Comparison of different combinations of feature selection methods and regression methods for time-series data based Spike antibody levels prediction.

Regression Method	FS method	MSE	RMSE	MAE	R^2
LSTM	**CatBoost**	**0.486**	**0.697**	**0.543**	**0.519**
	XGBoost	0.522	0.722	0.561	0.484
	LightGBM	0.498	0.705	0.542	0.507

V. Discussion

This study integrates the information of previous diseases, blood test results, and vital sign data, maximizing the utilization of data; the data have strengths such as big size, low missing values, and high quality. Since the clinical course, as well as the immunological reaction of COVID-19, is notable for its extreme variability, identifying the main associated factors might help understand the variability in patients.

Mueller et al. [9] used serum pro-inflammatory, anti-inflammatory, anti-viral cytokine, and anti-SARS-CoV-2 antibody measurements to cluster COVID-19 patients into three distinct immune phenotype groups by a machine learning approach. These immune-types reflect variations of immune response. Differing from [9] employing the unsupervised clustering, our work employs the supervised learning technology. There is another difference. [9] used COVID-19 immunotypes to predict clinical severity progression, while our work directly predicts clinical severity by serological indicators without antibody level. Guleken et al. [18] used Fourier Transform InfraRed and Raman spectroscopy to identify patients with different COVID infection time by random forest, C5.0, KNN, DNN, XGBoost, and SVM. It is noted that the DNN model has a low accuracy. Differing from [18] employing Fourier Transform InfraRed-Raman spectroscopy measurements, our work employs the simple serological indicators with a low acquisition cost. There is another difference. The class labels of [18] correspond to patients infected after 1, 3 and 6 months. However, our work directly uses the severity diagnosed by doctors as class label. Rosado et al. [19] trained machine learning classifiers with the multiplex data for identifying individuals with previous COVID-19 infection. Random forest algorithm got the best classification performance. Another work [20] also detected previous COVID-19 infection in children and adults. Differing from [19], [20] whose class labels correspond to individuals with or without previous COVID-19 infection, our work excludes individuals without COVID-19 infection. [19] used antibody responses to identify individual with previous infection, while our work predicts the disease condition without using antibody responses.

ALB is the most abundant circulating plasma protein, which negatively correlates with mortality risk in different populations. For every 2.5 g/L decrease in the ALB level, the risk of death is estimated to increase by 24 % to 56 % [21]. Our results show ALB is crucial for the severity and outcome of COVID-19. Early detection and appropriate intervention of COVID-19 patients with low levels of ALB can help decrease the risk of disease progression and death.

PLT is a valuable prognostic marker in our model. Recently, many studies have investigated the association between early decrease in PLT levels and mortality outcomes in COVID-19 patients during the progression of the disease. Zhao et al. [22] designed a generalized additive model and a generalized additive mixed model on 532 COVID-19 patients to compare the changes and trends in PLT over time between survivors and non-survivors. They concluded that changes in PLT can dynamically reflect the patient's physiological condition in the early stage. PLT levels in the non-survival group gradually

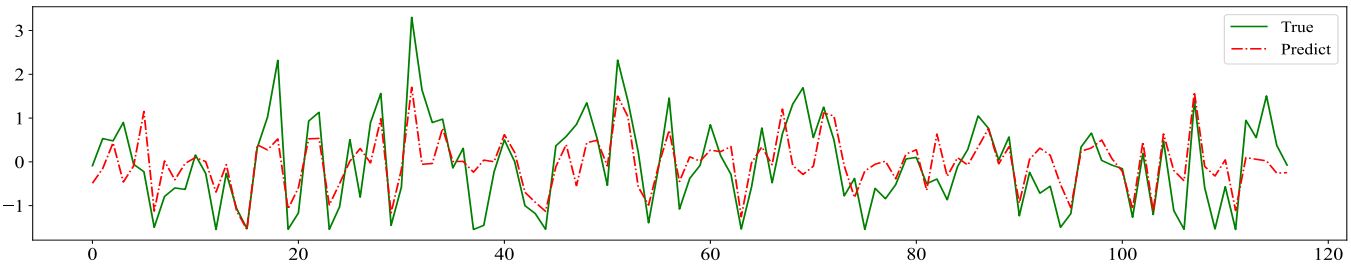

Fig. 13. Comparison of the true and the prediction of the method using CatBoost feature selection and LSTM regression for Spike antibody level prediction.

TABLE IX: Top-30 features for Spike antibody level prediction.

Algorithms	CatBoost		XGBoost		LightGBM
Variable	Importance	Variable	Importance	Variable	Importance
Age	1.000000	Age	1.000000	Age	1.000000
RDW_CV	0.490495	RDW_CV	0.749547	RDW_CV	0.568908
PLT	0.464925	PLT	0.746105	PLT	0.399160
LDH	0.344377	DM	0.614490	LDH	0.390756
eGFR(CKD-EPI)	0.317529	PCT	0.599591	eGFR(CKD-EPI)	0.374790
LYMPH(#)	0.293782	GLOB	0.529287	RDW_SD	0.367227
RDW_SD	0.269184	Eos(#)	0.430937	LYMPH(#)	0.349580
PCT	0.241220	Sex	0.427246	Eos(#)	0.315966
TCHO	0.226802	TCHO	0.400779	TCHO	0.301681
Eos(#)	0.213649	Cl	0.377002	γ-GT	0.296639
GLOB	0.182979	eGFR(CKD-EPI)	0.366495	Cl	0.292437
Sex	0.180278	LDH	0.349848	GLOB	0.275630
Na	0.172479	RDW_SD	0.296803	PCT	0.257983
MCH	0.170772	P-LCR	0.280620	MCH	0.219328
γ-GT	0.157314	MCHC	0.244588	MCHC	0.210924
DM	0.152515	MCH	0.218203	HCO	0.210084
TP	0.141478	RBC	0.216468	Urea	0.200000
Eos(%)	0.140449	PCV	0.215241	Na	0.198319
Cl	0.132038	PDW	0.210015	ALP	0.183193
UA	0.128401	HCO	0.205061	UA	0.174790
WBC	0.118042	TP	0.197185	RBC	0.161345
RBC	0.118038	γ-GT	0.185392	Ca	0.151261
Cre	0.117227	Cre	0.175898	ALB	0.151261
A/G	0.114586	LYMPH(#)	0.175799	Eos(%)	0.151261
HCO	0.112674	Na	0.173207	Sex	0.144538
PCV	0.111495	Urea	0.169811	TP	0.141176
MCV	0.106073	Eos(%)	0.168386	ALT	0.136134
Urea	0.103129	Eos(#)	0.161554	Cre	0.136134
P-LCR	0.097980	UA	0.157128	TBil	0.133613
Ca	0.097961	ALB	0.138300	K	0.131933

decreased, and that in the survival group gradually increased within one week after admission. Another observational study [23] characterized the dynamic changes of coagulation and platelet functions in COVID-19 patients. They noted that low PLT is associated with high risk of disseminated intravascular coagulation (DIC) and high mortality. The lower the PLT level is, the poorer the outcome is, and the higher mortality is [24]. Our experimental results also show PLT is crucial for the outcome of COVID-19. Change of PLT can serve as an early warning indicator for the treatment of COVID-19.

Although SARS-CoV-2 targets specific cells in the lung, it can also damage the kidney. Urea in the blood is reported as blood urea nitrogen (BUN), which can reflect the progression of kidney damage. A prospective cohort study [25] show that the BUN and AKI are significantly associated with in-hospital mortality, and elevated baseline BUN is an independent risk factor for in-hospital death. Cheng et al. [26] found that initial BUN can serve as a risk assessment tool. Li et al. [27] found that the lowest serum levels of Urea during hospitalization can be a marker of disease severity in COVID-19 patients. Our study includes Urea in the model, which ties nicely with the above studies.

CRP is a valuable biomarker. Its level will be abnormally elevated in the event of tissue damage or acute infection. COVID-19 is characterized by extensive pulmonary complications in the most severe cases, including acute lung injury (ALI) and acute respiratory distress syndrome (ARDS). Wang [28] compared the largest lung lesion diameter with CRP levels, and found that CRP levels are proportional to disease severity. Akdogan et al. [29] and Poggiali et al. [30] further found that the LDH and CRP levels can serve as potential predictors of COVID-19-related respiratory failure. The hypersensitive CRP (hs-CRP) test can detect protein at lower concentrations and has higher sensitivity, which is more effective than the conventional CRP test. Our study shows high level of hs-CRP is associated with high risk of severity disease and high mortality.

This paper gives the following new recommendations re-

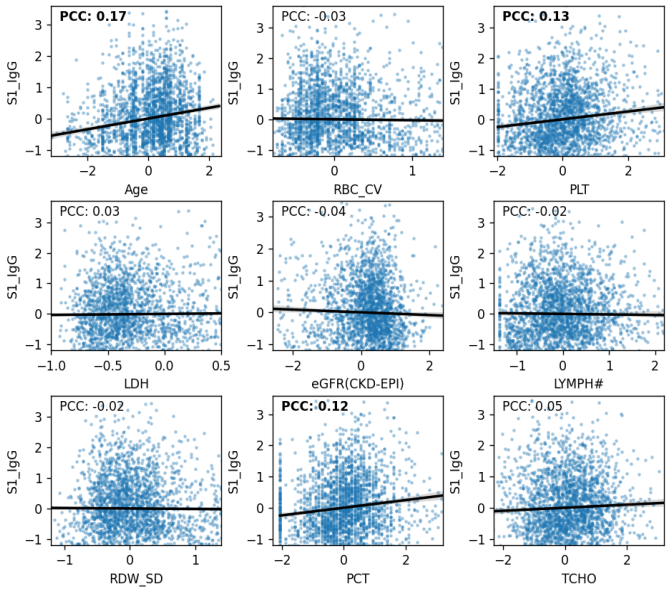

Fig. 14. The scatter plot between the Spike antibody level (S1_IgG) and the Top-9 features. PCC denotes the Pearson correlation coefficient between Spike antibody level and the feature. Bold fonts mean the PCC values are large and indicate strong correlations.

garding required blood test data for patients with suspected COVID-19. Firstly, ALB, PLT, and Urea have not yet been included in the latest Diagnosis and Treatment Protocol for COVID-19 of China [1]. However, our results shows ALB, PLT, and Urea are important markers for the prediction of disease severity and clinical outcome. It is recommended to further include ALB, PLT, and Urea to the general examination of COVID-19 diagnosis. It is advisable for patients with suspected COVID-19 who have abnormal ALB, PLT, or Urea to consider further inspection. Secondly, the latest Protocol [1] points out that only a limited portion of COVID-19 infected patients have elevated CRP levels. Our results show that hs-CRP is a critical factor for clinical outcome prediction. Replacing CRP detection with hs-CRP detection in clinical examination may improve the success rate of screening for COVID-19 infected patients. Thirdly, patients with suspected COVID-19 are advised to use AI and the examination results of LDH, Mono%, ALB, LYMPH%, LDH, Neu#, hs-CRP, PLT, and Urea for determining whether to proceed with the next step of examination and treatment.

This research has the following shortcomings. Firstly, the proposed models assume equal intervals between routine blood tests for each patient. Therefore, the model may not describe the irregular sampling interval. Secondly, our data are obtained from unvaccinated patients with SARS-CoV-2 infection, so the proposed models may not be applicable to vaccinated patients and patients with mutated strains of infection.

VI. Conclusion and Future Work

The prediction models based on LSTM provide a new reference for the diagnosis and prognosis of COVID-19 patients. We introduce TA block to enhance the global temporal dependencies in clinical outcome prediction, which leads to significant performance improvements with a small increase of computational cost. Simple factors like LDH, Mono%, ALB, LYMPH%, DM, and Sex are critical factors in disease severity. LDH, Neu#, hs-CRP, PLT, and Urea are critical factors in clinical outcomes. We further find that Age, RDW_CV, PLT, LDH, eGFR(CKD-EPI), LYMPH#, RDW_SD, PCT, and TCHO are the Top-9 significant predictors of the Spike antibody level. Our future work will include handling imbalanced data and improving LSTM to model the irregularity of sampling intervals. We look forward to the availability of the large-sample data of Omicron-infected patients.

Appendix A. Supplementary Materials

The supplementary materials and codes are available at https://github.com/OmaZio2/covid-19-coding.

We have provided a comparison of admission/discharge characteristics of the COVID-19 patients. We have performed the correlation analysis between serological indicators and disease severity / clinical outcome / S1_IgG levels both at the admission time and the discharge time. The correlation analysis results are available at https://yi0rst.axshare.com/. The preliminary analysis results show that most collected serological indicators have the same correlation with disease severity, clinical outcome, and S1_IgG levels both at admission and discharge. This character allows us to combine the admission and discharge samples for developing the model.

The tested serological indicators include Hemoglobin (HGB), Absolute value of lymphocytes (LYMPH#), Percentage of lymphocytes (LYMPH%), Mean corpuscular hemoglobin (MCH), Mean corpuscular hemoglobin concentration (MCHC), Mean corpuscular volume (MCV), Absolute value of monocyte (Mono#), Percentage of monocyte (Mono%), Absolute value of neutrophil granulocyte (Neu#), Percentage of neutrophil granulocyte (Neu%), Platelet count (PLT), Erythrocyte Count (RBC), Absolute value of basophil (Baso#), Percentage of basophil (Baso%), Absolute value of eosinophilic (Eos#), Percentage of eosinophilic (Eos%), Hematokrit (HCT), White blood cell count (WBC), Red cell volume distribution width SD (RDW_SD), Red cell volume distribution width CV (RDW_CV), Mean platelet volume (MPV), Platelet distribution width (PDW), Platelet large cell ratio (P-LCR), PCT, K, Ca, Na, Cl, Aspartate aminotransferase (AST), Lactic dehydrogenase (LDH), Lactic dehydrogenase*0.9 (LDH*0.9), Glutamic pyruvic transaminase (ALT), Total cholesterol (TCHO), Albumin (ALB), Alkaline phosphatase (ALP), γ-glutamyl transpeptidase (γ-GT), Total bilirubin (TBil), Total protein (TP), Ratio of albumin to globulin (A/G), Globulin (GLOB), Total protein*0.75 (TP*0.75), Direct Bilirubin (BC), Total bilirubin*0.8 (TBil*0.8), Indirect bilirubin (IBil), Creatinine (Cre), Urea, Uric acid (UA), Bicarbonate (HCO), Epidermal growth factor receptor based on CKD-EPI equation (eGFR(CKD-EPI)), Calcium Correction (CC), Hypersensitive C-reactive protein (hs-CRP), D-Dimer, Prothrombin time (PT), Prothrombin activity (PTA), International normalized ratio (INR), Activated partial thromboplastin time (APTT), Fibrinogen (FIB), Thrombin time (TT), Glucose (GLU), High-sensitive cardiac troponin I (hs-cTnI), N terminal

pro B type natriuretic peptide (NT-proBNP), Interleukin-6 (IL-6), Ferritin (FER), Creatine kinase (CK), Interleukin-1β (IL-1β), Interleukin-2 Receptors (IL-2R), Interleukin-8 (IL-8), Interleukin-10 (IL-10), Tumor necrosis factor-α (TNF-α), Triglyceride (TG), Mg, P, Antithrombin (AT), Low-density lipoprotein (LDL-C), High-density lipoprotein (HDL-C), Low-density lipoprotein+High-density lipoprotein (LDL-C+HDL-C), Fibrinogen Degradation Products (FDP), Myoglobin (Mb), Creatine Kinase MB Form (CK-MB), Total bile acids (TBA1), Cholinesterase (CHE), Prealbumin (PAB), α-L-fucosidase (AFU), Erythrocyte sedimentation rate (ESR), Cystatin C (Cys C), Amylase (Amy), and Glutamate dehydrogenase (GDH).

REFERENCES

[1] N. H. C. of China and N. T. Administration, "Diagnosis and treatment protocol for covid-19 patients (trial version 10)," *Infectious Microbes & Diseases*, vol. 1, no. 01, pp. 3–12, 2023.

[2] A. Saood and I. Hatem, "Covid-19 lung ct image segmentation using deep learning methods: U-net versus segnet," *BMC Medical Imaging*, vol. 21, no. 1, pp. 1–10, 2021.

[3] L. Li, L. Qin, Z. Xu, Y. Yin, X. Wang, B. Kong, J. Bai, Y. Lu, Z. Fang, Q. Song *et al.*, "Artificial intelligence distinguishes covid-19 from community acquired pneumonia on chest ct," *Radiology*, 2020.

[4] F. A. Mettler, W. Huda, T. T. Yoshizumi, M. Mahesh *et al.*, "Effective doses in radiology and diagnostic nuclear medicine: a catalog," *Radiology*, vol. 248, no. 1, p. 254, 2008.

[5] M. Kukar, G. Gunar, T. Vovko, S. Podnar, and M. Notar, "Covid-19 diagnosis by routine blood tests using machine learning," *Scientific reports*, vol. 11, no. 1, p. 10738.

[6] A. A. Soltan, S. Kouchaki, T. Zhu, D. Kiyasseh, T. Taylor, Z. B. Hussain, T. Peto, A. J. Brent, D. W. Eyre, and D. A. Clifton, "Rapid triage for covid-19 using routine clinical data for patients attending hospital: development and prospective validation of an artificial intelligence screening test," *The Lancet Digital Health*, vol. 3, no. 2, pp. e78–e87, 2021.

[7] W.-j. Guan, Z.-y. Ni, Y. Hu, W.-h. Liang, C.-q. Ou, J.-x. He, L. Liu, H. Shan, C.-l. Lei, D. S. Hui *et al.*, "Clinical characteristics of coronavirus disease 2019 in china," *New England journal of medicine*, vol. 382, no. 18, pp. 1708–1720, 2020.

[8] N. Lee, P. Chan, M. Ip, E. Wong, J. Ho, C. Ho, C. Cockram, and D. S. Hui, "Anti-sars-cov igg response in relation to disease severity of severe acute respiratory syndrome," *Journal of clinical virology*, vol. 35, no. 2, pp. 179–184, 2006.

[9] Y. Mueller, T. Schrama, R. Ruijten, M. Schreurs, D. Grashof, H. van de Werken, G. Jona Lasinio, D. Alvarez-de la Sierra, C. Kiernan, M. Eiro, M. Meurs, I. Brouwers-Haspels, Z. Manzhi, L. Li, H. Wit, C. Ouzounis, M. Wilmsen, T. Alofs, D. Laport, and P. Katsikis, "Stratification of hospitalized covid-19 patients into clinical severity progression groups by immuno-phenotyping and machine learning," *Nature Communications*, vol. 13, p. 915, 02 2022.

[10] X. Yan, G. Chen, Z. Jin, Z. Zhang, B. Zhang, J. He, S. Yin, J. Huang, M. Fan, Z. Li *et al.*, "Anti-sars-cov-2 igg levels in relation to disease severity of covid-19," *Journal of medical virology*, vol. 94, no. 1, pp. 380–383, 2022.

[11] Y. Guo, T. Li, X. Xia, B. Su, H. Li, Y. Feng, J. Han, X. Wang, L. Jia, Z. Bao *et al.*, "Different profiles of antibodies and cytokines were found between severe and moderate covid-19 patients," *Frontiers in Immunology*, p. 3344, 2021.

[12] B. Zhang, X. Zhou, C. Zhu, Y. Song, F. Feng, Y. Qiu, J. Feng, Q. Jia, Q. Song, B. Zhu *et al.*, "Immune phenotyping based on the neutrophil-to-lymphocyte ratio and igg level predicts disease severity and outcome for patients with covid-19," *Frontiers in molecular biosciences*, vol. 7, p. 157, 2020.

[13] A. Embaby, M. G. Hamed, H. F. Ebian, L. A. El-Korashi, M. Walaa, E. M. A. El-Sattar, A. S. Hanafy, and S. Abdelmoneem, "Clinical utility of haematological inflammatory biomarkers in predicting 30-day mortality in hospitalised adult patients with covid-19," *British Journal of Haematology*, vol. 200, pp. 708 – 716, 2022.

[14] A. Shankaralingappa, S. Tummidi, and T. A. Babu, "Diagnostic value of platelet indices in covid 19 infection: a case-control study from a single tertiary care center," *The Egyptian Journal of Internal Medicine*, vol. 34, 2022.

[15] A. Mirijello, P. Piscitelli, A. de Matthaeis, M. Inglese, M. M. D'Errico, V. Massa, A. Greco, A. Fontana, M. Copetti, L. Florio *et al.*, "Low egfr is a strong predictor of worse outcome in hospitalized covid-19 patients," *Journal of Clinical Medicine*, vol. 10, no. 22, p. 5224, 2021.

[16] E. Nader, C. Nougier, C. Boisson, S. Poutrel, J. Catella, F. G. Martin, J. Charvet, S. Girard, S. Havard-Guibert, M. Martin, H. Rezigue, H. Desmurs-Clavel, C. Renoux, P. Joly, N. Guillot, Y. Bertrand, A. Hot, Y. Dargaud, and P. Connes, "Increased blood viscosity and red blood cell aggregation in patients with covid-19," *American Journal of Hematology*, vol. 97, pp. 283 – 292, 2021.

[17] C. Wang, R. Deng, L. Gou, Z. Fu, X. Zhang, F. Shao, G. Wang, W. Fu, J. Xiao, X. Ding *et al.*, "Preliminary study to identify severe from moderate cases of covid-19 using combined hematology parameters," *Annals of translational medicine*, vol. 8, no. 9, 2020.

[18] Z. Guleken, Y. Tuyji Tok, P. Jakubczyk, W. Paja, K. Pancerz, Y. Shpotyuk, J. Cebulski, and J. Depciuch, "Development of novel spectroscopic and machine learning methods for the measurement of periodic changes in covid-19 antibody level," *Measurement*, vol. 196, p. 111258, 2022.

[19] J. Rosado, S. Pelleau, C. Cockram, S. H. Merkling, N. Nekkab, C. Demeret, A. Meola, S. Kerneis, B. Terrier, S. Fafi-Kremer, J. de Seze, T. Bruel, F. Dejardin, S. Petres, R. Longley, A. Fontanet, M. Backovic, I. Mueller, and M. T. White, "Multiplex assays for the identification of serological signatures of sars-cov-2 infection: an antibody-based diagnostic and machine learning study," *The Lancet Microbe*, vol. 2, no. 2, pp. e60–e69, 2021.

[20] A. Thomas, E. Oliver, B. HE, and at al., "Evaluation and deployment of isotype-specific salivary antibody assays for detecting previous sars-cov-2 infection in children and adults," *Commun Med (Lond)*, vol. 3, no. 1, p. 37, 2023.

[21] P. Goldwasser and J. Feldman, "Association of serum albumin and mortality risk," *Journal of clinical epidemiology*, vol. 50, no. 6, pp. 693–703, 1997.

[22] X. Zhao, K. Wang, P. Zuo, Y. Liu, M. Zhang, S. Xie, H. Zhang, X. Chen, and C. Liu, "Early decrease in blood platelet count is associated with poor prognosis in covid-19 patients—indications for predictive, preventive, and personalized medical approach," *EPMA Journal*, vol. 11, no. 2, pp. 139–145, 2020.

[23] C. Bao, X. Tao, W. Cui, B. Yi, T. Pan, K. H. Young, and W. Qian, "Sars-cov-2 induced thrombocytopenia as an important biomarker significantly correlated with abnormal coagulation function, increased intravascular blood clot risk and mortality in covid-19 patients," *Experimental Hematology & Oncology*, vol. 9, no. 1, pp. 1–8, 2020.

[24] X. Yang, Q. Yang, Y. Wang, Y. Wu, J. Xu, Y. Yu, and Y. Shang, "Thrombocytopenia and its association with mortality in patients with covid-19," *Journal of Thrombosis and Haemostasis*, vol. 18, no. 6, pp. 1469–1472, 2020.

[25] Y. Cheng, R. Luo, K. Wang, M. Zhang, Z. Wang, L. Dong, J. Li, Y. Yao, S. Ge, and G. Xu, "Kidney disease is associated with in-hospital death of patients with covid-19," *Kidney international*, vol. 97, no. 5, pp. 829–838, 2020.

[26] A. Cheng, L. Hu, Y. Wang, L. Huang, L. Zhao, C. Zhang, X. Liu, R. Xu, F. Liu, J. Li *et al.*, "Diagnostic performance of initial blood urea nitrogen combined with d-dimer levels for predicting in-hospital mortality in covid-19 patients," *International journal of antimicrobial agents*, vol. 56, no. 3, p. 106110, 2020.

[27] G. Li, X. Wu, C.-l. Zhou, Y.-m. Wang, B. Song, X.-b. Cheng, Q.-f. Dong, L.-l. Wang, S.-s. You, and Y.-m. Ba, "Uric acid as a prognostic factor and critical marker of covid-19," *Scientific Reports*, vol. 11, no. 1, pp. 1–9, 2021.

[28] L. Wang, "C-reactive protein levels in the early stage of covid-19," *Medecine et maladies infectieuses*, vol. 50, no. 4, pp. 332–334, 2020.

[29] D. Akdogan, M. Guzel, D. Tosun, and O. Akpinar, "Diagnostic and early prognostic value of serum crp and ldh levels in patients with possible covid-19 at the first admission," *The Journal of Infection in Developing Countries*, vol. 15, no. 06, pp. 766–772, 2021.

[30] E. Poggiali, D. Zaino, P. Immovilli, L. Rovero, G. Losi, A. Dacrema, M. Nuccetelli, G. B. Vadacca, D. Guidetti, A. Vercelli *et al.*, "Lactate dehydrogenase and c-reactive protein as predictors of respiratory failure in covid-19 patients," *Clinica chimica acta*, vol. 509, pp. 135–138, 2020.